

Numerical Modelling and Analysis of Turbulent Flow in an Open Channel with Submerged Vegetation

D. Kasiteropoulou¹ · A. Liakopoulos¹ · N. Michalolias¹ · E. Keramaris¹

Received: 5 December 2016 / Accepted: 25 April 2017 / Published online: 9 May 2017
© Springer International Publishing Switzerland 2017

Abstract Turbulent flow in an open channel whose bed is covered with vegetation is studied. Vegetation has been modeled by a series of small diameter rigid cylinders protruded vertically from the channel bed. 3-D computations were performed using the ANSYS-CFX computer program which uses a finite volume method to solve the partial differential equations describing fluid flow. In order to reduce the computational burden, periodic boundary conditions in the direction of the channel axis have been used. The computational domain has been discretized using tetrahedral elements. Six mesh designs were evaluated in order to choose the optimal/suboptimal mesh and ensure that the solution is independent of the mesh used. The mesh finally chosen provides a good balance between the stability of the solution and the flow field resolution. However, achieving mesh-independent solutions for a complex geometry problem, such as the one studied in this work, requires tremendous computational resources. The connection of the hydrodynamic model to the study of contaminant transport and sedimentation processes in aquatic environments is also discussed.

Keywords Free-surface flow · Channel vegetation model · Turbulent flow · ANSYS-CFX computer package

1 Introduction

Vegetation constitutes one of the more important factors that impact the turbulent flow in natural open channels as well as the transport processes of sediments, influencing the operation of wetlands and the flood areas of rivers. The existence of aquatic plants causes increase of resistance in the flow and simultaneous reduction of mean velocity in comparison with areas without vegetation. The interaction between the type of vegetation and characteristics of flow

✉ A. Liakopoulos
aliakop@uth.gr

¹ Hydromechanics and Environmental Engineering Laboratory, Department of Civil Engineering, University of Thessaly, Pedion Areos, 38334 Volos, Greece

field is of great interest in the planning and design of flood protection systems. Furthermore, there is a tendency in the current scientific literature to proceed from simple hydraulic models to more complex models that include hydrodynamic and eco-hydraulic considerations (Nepf 2012; Nepf and Ghisalberti 2008; Katul et al. 2011; Nikora 2010). In this respect, distinction has to be made between modeling rivers and wetlands as discussed in Kucukali and Cokgor (2006), Tsihrintzis and Madiedo (2000), and Wilson et al. (2006).

A number of studies appeared in the technical literature during the last 20 years, regarding the effect of vegetation in channels with free surface (Wilson et al. 2003; Liu et al. 2008; Stoesser et al. 2010; Huai et al. 2009; Okamoto and Nezu 2010; Marjoribanks et al. 2016). Klopstra et al. (1997) and Meijer and van Velzen (1999) developed a method for the determination of velocity profile that separates the area of flow in two layers, the one inside and the other above the vegetation. Their theory was supported from the momentum equation in the vegetation layer and simultaneously maintained the logarithmic profile in the above part (method of two layers).

In the study of Fisher-Antze et al. (2001), velocity distributions have been computed using a three-dimensional model in channels partially covered with vegetation. The Navier-Stokes equations were solved, using the SIMPLE method and the $k-\epsilon$ turbulence model. The vegetation was modelled as vertical cylinders. The numerical model was tested against three laboratory experiments using straight flumes with uniform flow, where vegetation partially covered the cross-section. The velocity and vegetation density varied in both vertical and horizontal directions in the different cases. The experiments also included varying cross-sectional shapes. All tests gave fairly good correspondence between computed and measured velocity profiles.

Lopez and Garcia (2001) developed a model for the calculation of mean velocities and the characteristics of turbulent flow in open channel with vegetation. Their theory was based on the fact that the resistance because of the vegetation is taken into consideration not only in the momentum equation, but also in the equations of modified model $k-\epsilon$. The similarity of these two models is due to the fact that the initial approach was for aquatic vegetation, but there exists a possibility of extension and in submerged vegetation. Defina and Bixio (2005) modified the two mentioned models to examine the geometry of plants and the factor of resistance in connection with the flow depth. In their theory, they added the equation of turbulent kinetic energy for the model of two layers.

Wilson et al. (2006) used a 3-D program of finite elements (SSIM) for the study of influence of vegetation on the velocity distribution. This model resolves the momentum and continuity equations for each element and uses the $k-\epsilon$ model in modeling turbulence.

Cui and Neary (2008) used large eddy simulation (LES) to show how the vegetation significantly changes the mean flow, Reynolds shear stress, turbulence intensities, turbulence event frequencies, and the flow energy budget within and above the vegetation layers.

In the study of Erduran (2012), the construction of an integrated numerical model to deal with the interactions between vegetated surface and saturated subsurface flows was presented. A numerical model was built by integrating the previously developed quasi-three-dimensional (Q3D) vegetated surface flow model with a two-dimensional (2D) saturated groundwater flow model. The vegetated surface flow model was constructed by coupling the explicit finite volume solution of 2D shallow water equations (SWEs) with the implicit finite difference solution of Navier-Stokes equations (NSEs) for vertical velocity distribution. The subsurface model was based on the explicit finite volume solution of 2D saturated groundwater flow equations (SGFEs).

In this study, the results of modeling flow in an open channel whose bed is covered with vegetation, using Computational Fluid Dynamics (CFD) methods, are presented. Vegetation has been modeled by a series of small diameter cylinders which protrude vertically from the

channel bed. In order to reduce the computational burden, periodic boundary conditions in the direction of the channel axis have been used. The computational domain has been discretized using tetrahedral elements. Six mesh designs were evaluated. The simulation was performed using the computational program ANSYS-CFX which employs the method of finite volumes for the solution of fluid mechanics equations. The results from this computational study were compared with laboratory measurements and a good agreement between experiments and computational model regarding the qualitative characteristics of flow was found.

2 Mathematical Model and Numerical Approach

2.1 Mathematical Model

The mathematical model of the turbulent flow in this work consists of the Reynolds-Averaged Navier-Stokes (RANS) equations coupled with the $k-\varepsilon$ turbulence model. Each primitive flow variable is decomposed to an averaged-in-time part and a fluctuation term. For example, the velocity vector at a point in the flow field is given as the sum of the time-averaged velocity $\overline{\vec{U}}$ and a time-dependent velocity fluctuation \vec{u}' , i.e., we write

$$\vec{U} = \overline{\vec{U}} + \vec{u}' \quad (1)$$

The time-averaged velocity vector is defined as

$$\overline{\vec{U}} = \frac{1}{\Delta t} \int_t^{t+T} \vec{U} dt \quad (2)$$

where T is a time interval much longer than the characteristic periods of the turbulence fluctuations. The use of mean values (in time) in the conservation equations leads to the Reynolds-Averaged Navier-Stokes (RANS) equations:

$$\frac{\partial \rho}{\partial t} + \nabla \cdot (\rho \overline{\vec{U}}) = 0 \quad (3)$$

$$\frac{\partial \rho \overline{\vec{U}}}{\partial t} + \nabla \cdot (\rho \overline{\vec{U}} \otimes \overline{\vec{U}}) = \nabla \cdot (\tau - \rho \overline{\vec{u}' \otimes \vec{u}'}) + \vec{S}_M \quad (4)$$

In Eq. (4), $\overline{\rho \vec{u}' \otimes \vec{u}'}$ are the Reynolds stresses and τ denotes the stress tensor due to molecular viscosity.

After introducing the concept of an effective viscosity, μ_{eff} , the conservation of mass equation is unchanged.

and the conservation of momentum equation is written as

$$\frac{\partial \rho \overline{\vec{U}}}{\partial t} + \nabla \cdot (\rho \overline{\vec{U}} \otimes \overline{\vec{U}}) - \nabla \cdot (\mu_{eff} \nabla \overline{\vec{U}}) = -\nabla p' + \nabla \cdot (\mu_{eff} \nabla \overline{\vec{U}})^T + \vec{b} \quad (5)$$

where \vec{b} is the total body force per unit mass, μ_{eff} is the effective viscosity and p' is the modified pressure defined as

$$p' = p + \frac{2}{3} \rho k + \nabla \cdot \vec{U} \left(\frac{2}{3} \mu_{eff} - \zeta \right) \tag{6}$$

In Eq. (6), ζ is the fluid bulk viscosity, ρ is the fluid density and k denotes the turbulent kinetic energy.

The k- ϵ model is used in this work for the calculation of the turbulent viscosity at each point of the flow field. The k- ϵ model is a two differential equation model where the effective viscosity is calculated as the sum of turbulent viscosity (μ_t) and molecular viscosity (μ) i.e.,

$$\mu_{eff} = \mu + \mu_t \tag{7}$$

The turbulent viscosity is computed at each point of the flow field in terms of the turbulence kinetic energy, k , and the turbulence kinetic energy dissipation rate, ϵ , by the relation

$$\mu_t = C_\mu \rho \frac{k^2}{\epsilon} \tag{8}$$

where $C_\mu = 0.09$.

The required values of k and ϵ are computed at each point of the turbulent flow field by concurrently solving the following two partial differential equations (Liakopoulos 2010):

$$\frac{\partial(\rho k)}{\partial t} + \nabla \cdot \left(\rho \vec{U} k \right) = \nabla \cdot \left[\left(\mu + \frac{\mu_t}{\sigma_k} \right) \nabla k \right] + P_k - \rho \epsilon \tag{9}$$

$$\frac{\partial(\rho \epsilon)}{\partial t} + \nabla \cdot \left(\rho \vec{U} \epsilon \right) = \nabla \cdot \left[\left(\mu + \frac{\mu_t}{\sigma_\epsilon} \right) \nabla \epsilon \right] + \frac{\epsilon}{k} (C_{e1} P_k - C_{e2} \rho \epsilon) \tag{10}$$

where $C_{e1} = 1.45$, $C_{e2} = 1.90$, $\sigma_k = 1.00$, $\sigma_\epsilon = 1.30$ and P_k is the rate of production of turbulence kinetic energy calculated by

$$P_k = \mu_t \nabla \vec{U} \cdot \left(\nabla \vec{U} + \nabla \vec{U}^T \right) - \frac{2}{3} \nabla \cdot \vec{U} \left(3 \mu_t \nabla \cdot \vec{U} + \rho k \right) \tag{11}$$

The ANSYS-CFX computer package is used in this work under the assumption of incompressible flow with constant properties ($\rho = \text{constant}$, $\mu = \text{constant}$) and bulk viscosity $\zeta = 0$.

2.2 Vegetation Model

In setting up a vegetation model, a number of parameters has to be chosen such as shape, height, vegetation density, and flexibility (or rigidity) of the plants. Dunn et al. (1996) performed a series of laboratory experiments at the University of Illinois aiming at describing channel flow with free surface as well as the calculation of resistance caused by bed vegetation. The measurements were performed in a tilting flume (the slope was varied from 0.0036 to 0.0161) of length 19.5 m, width of 0.91 m and depth of 0.61 m. The plants were simulated with flexible or inflexible cylinders. Experiment No. 12 of the Illinois group (Discharge $Q = 0.181 \text{ m}^3/\text{s}$, Froude number $Fr = 0.58$

(subcritical flow), cylinder density $a = 0.62 \text{ m}^{-1}$, which expresses the density of vegetation, channel slope $s = 0.011$ has been discussed in the literature. Stamou et al. (2012), based on the Illinois experiment setup, simulated numerically experiment No. 12 using ANSYS-CFX. More specifically, the flow was numerically simulated using a computational domain of length 2.0 m, width 0.91 m and flow depth 0.233 m. Plant stems were modelled as rigid cylinders of diameter 0.00635 m and height of 0.118 m.

In the present study, an attempt was made to minimize the computational burden. To this end, we simulated the flow in two rows of cylinders formed as in the work of Dunn et al. (1996), experiment No. 12, using periodic boundary conditions in the main flow direction. Consequently, our computational domain has a length of 0.2032 m. The first line of cylinders begins at a distance 0.0508 m from the vertical channel side wall and the other is shifted by 0.1016 m (see Fig. 1). In total, 17 cylinders (9 in the first line and 8 in the next) were placed. The other geometrical parameters of the model were chosen as in Stamou et al. (2012).

As shown in Fig. 1, the x-y plane in our work coincides with the channel bed and the origin of the coordinate system is at the center of the computational domain. A 3-D (isometric) view of the computational domain is shown in Fig. 2a. The blue solid surfaces simulate the bed vegetation modelled as rigid cylinders.

2.3 Boundary Conditions and Mesh Design

In order to complete the mathematical model, free slip boundary condition was specified at the free surface. All channel and cylinder solid walls were assumed smooth without slip velocity (no-slip boundary condition). A 3-D view of the mesh generated using the ANSYS-CFX preprocessor is shown in Fig. 2b.

To achieve grid independence, a sequence of mesh designs was used. Initially, a sparse grid was used which was then refined as shown in Table 1. A maximum edge length equal to 0.05 m and a minimum edge length 0.001 m were chosen in order to resolve the boundary layers formed near all solid surfaces. Sensitivity to global quantities, such as mass conservation was helpful in judging approximate convergence of the solutions.

3 Numerical Results

Various aspects of the computed 3-D velocity field are presented in Figs. 3, 4, 5, 6, 7, and 8. The calculated velocity vector field is shown in Fig. 3. The result presented is based on the coarse grid (Mesh 1) for clarity of the vector plot.

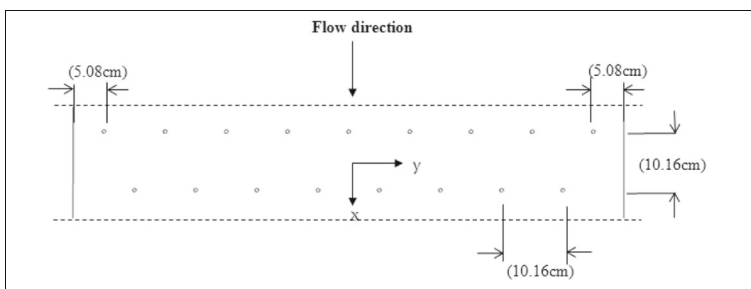


Fig. 1 Computational domain. Cylinder arrangement at the channel bed (Top view)

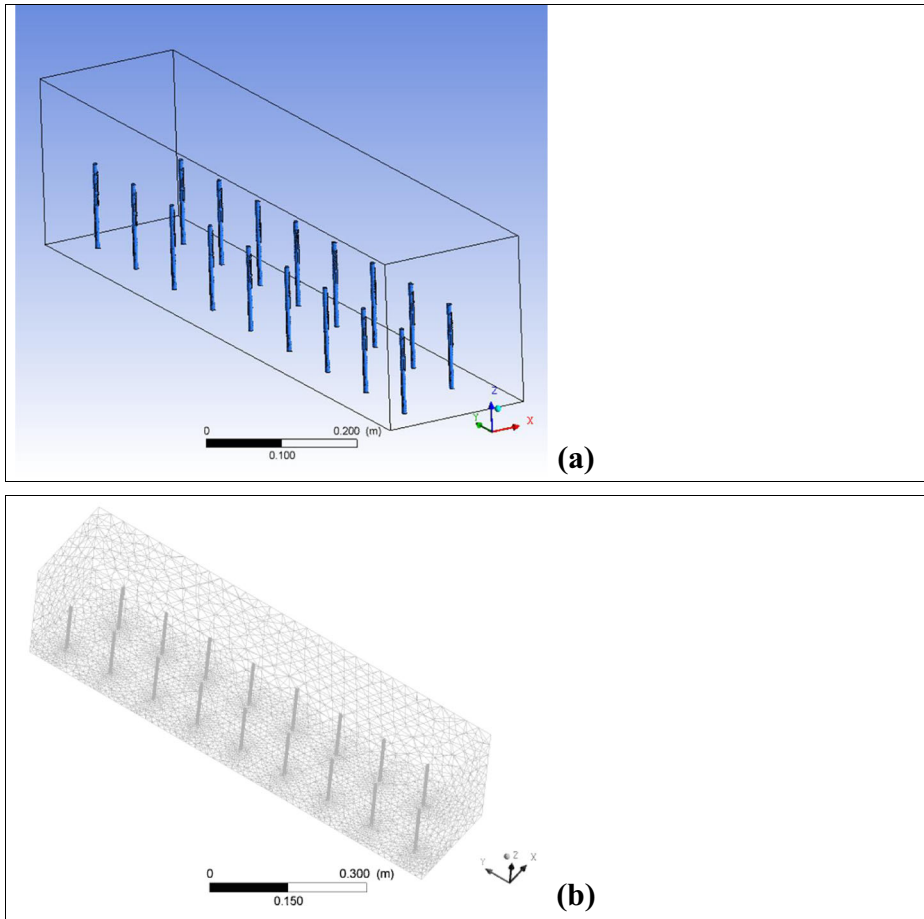


Fig. 2 **a** A 3-D view of the vegetated channel as modeled in the ANSYS-CFX environment. The main flow direction is along the x-axis; **b** A 3-D view of the mesh in the ANSYS-CFX environment

Contour plots of the velocity magnitude at five vertical planes ($x = -0.1016$ m, $x = 0.1016$ m, $x = 0$, $x = -0.0508$ m and $x = 0.0508$ m) are shown in Fig. 4. Figure 4a is presented here as a numerical check on how well the translational periodicity condition in the x-direction is enforced. We remind the reader that the coordinate system used in this work is defined in Fig. 1. Near the solid walls, the velocity profile is significantly affected and sharply lower velocities are observed very close to the walls. The region very close to the wall exhibits a nearly linear velocity profile in the

Table 1 Mesh parameters

	Number of nodes	Number of tetrahedra
Mesh 1	21035	77966
Mesh 2	21504	79322
Mesh 3	23195	84616
Mesh 4	27717	100086
Mesh 4n	62087	349329
Mesh 4n2	165480	938141

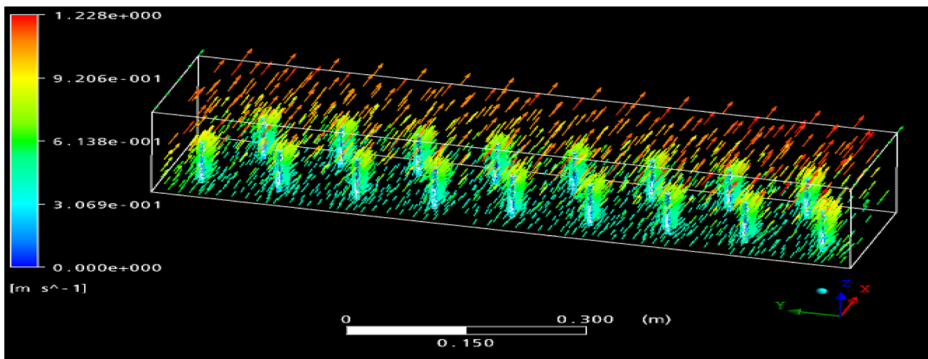


Fig. 3 Velocity vector field (Mesh 1). Mass flow rate: 181 kg/s, volume flow rate $Q = 0.181 \text{ m}^3/\text{s}$, Mean velocity = 0.850 m/s

turbulent case, and is completely dominated by viscous effects. It should be noted that in order to accurately resolve the boundary layers, an extremely fine grid must be used and, even if the resolution is adequate, the mean (in time) turbulent velocity profile is not modeled adequately when wall functions are used in the implementation of the $k-\epsilon$ model. For a discussion on $k-\epsilon$ model modification in order to resolve the boundary layer up to the solid wall, see Liakopoulos (1985).

In Fig. 5, contour plots of the x -velocity component are shown at two horizontal planes ($z = 0.05 \text{ m}$ and $z = 0.10 \text{ m}$) that intersect the rigid cylinders. Vortices are observed, as expected, in the region behind the cylinders (cylinder wakes). The formation is more pronounced as we move towards the top of the cylinders. We note that for the pattern of the cylinders studied and the chosen distances between cylinders, the wakes behind the cylinders interact weakly, see Michalolias (2014).

The velocity profiles computed with meshes employed in the present study exhibit the same qualitative behavior. A comparison of the computed vertical velocity profiles along the line segment $(0,0,0)$ to $(0,0, 0.223 \text{ m})$ is shown in Fig. 6. As we can see, significant differences exist, especially in the bottom layer in the submerged cylinder region. Stamou et al. (2012) have reported similar difficulties in achieving grid independence for the same problem although they have used very fine grids and a much larger computational domain (see Fig. 7).

In Fig. 6a, we present dimensional velocity profiles computed with meshes: grid4, grid 4n and grid 4n2. Although all profiles capture qualitatively the main characteristics of the mean flow, it is obvious that grid independent solution has not been achieved. There is no evidence of approaching convergence as the grid becomes finer. This is in agreement with the results reported by Stamou et al. (2012). We can speculate on the causes of this behaviour of the numerical solution. First of all, assigning value to the mass flow rate instead of specifying a known velocity distribution at the inlet of the computational domain is known to be a difficult problem in CFD. Second, the comparison of the vertical velocity profiles along the vertical line segment $(0, 0, 0)$ to $(0, 0, 0.233 \text{ m})$ is quite demanding test for convergence. It is located in the wake of the middle cylinder of the first row. Third, the generation of an appropriate grid for the problem at hand is rather tricky and a poor mesh design may be the explanation of not being able to reach grid independent solutions. Things look better if we plot profiles of the dimensionless velocity u/u_{\max} (see Fig. 6). If we think in the framework of a two-layer conceptual model for the flow under study, we see that in the upper layer the profiles collapse satisfactorily. The main difficulty appears in the lower layer (the vegetation layer) where even the non-dimensionalized profiles differ considerably. A non-dimensionalization with reference

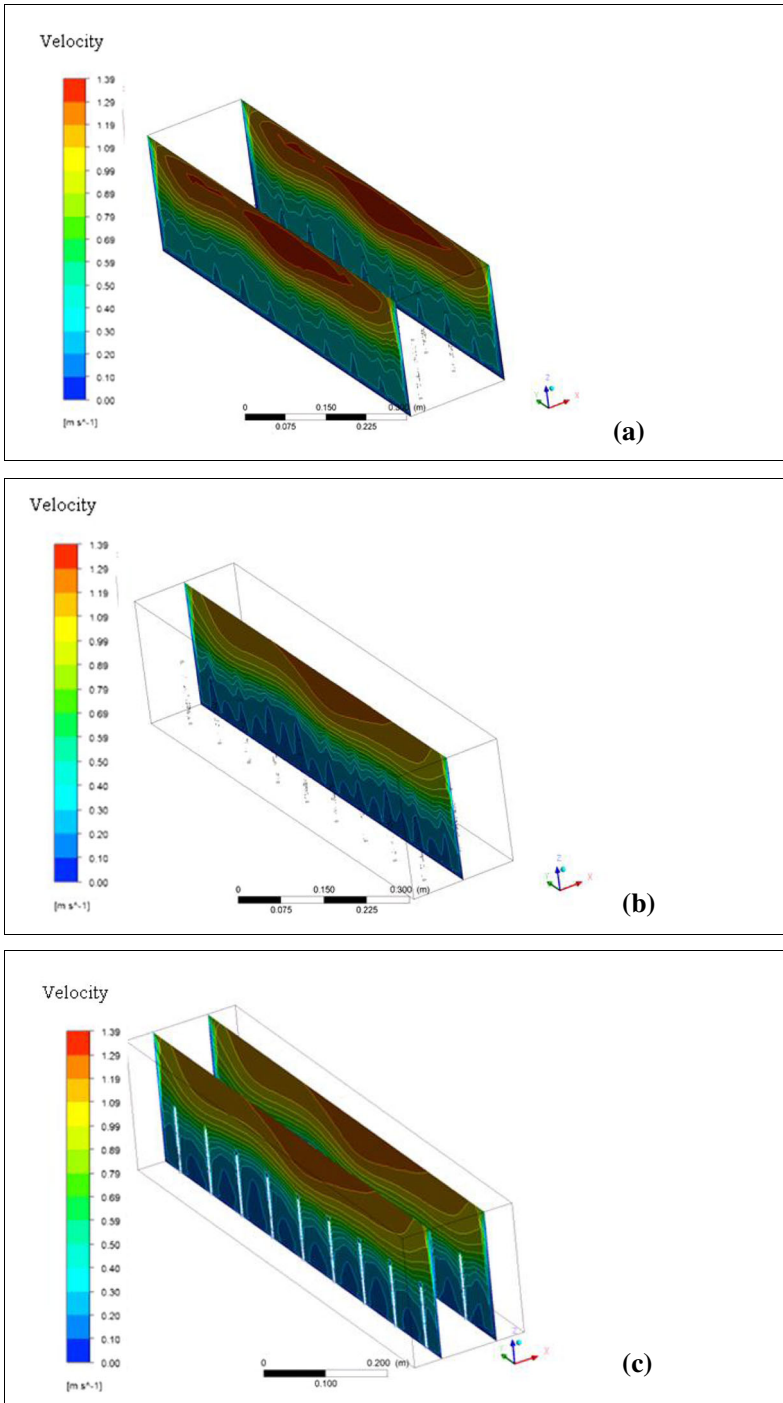


Fig. 4 Fluid speed distribution on planes (a) $x = -0.1016$ m and $x = 0.1016$ m; (b) $x = 0$; (c) $x = -0.0508$ m and $x = 0.0508$ m. Mass flow rate: 181 kg/s, volume flow rate $Q = 0.181$ m^3/s , Mean velocity = 0.850 m/s

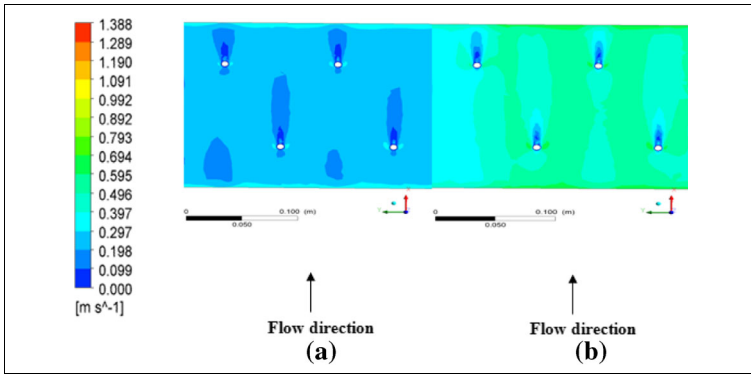


Fig. 5 Contour plots of speed velocity at various depths. (a) $z = 0.05$ m, (b) $z = 0.10$ m. Mass flow rate: 181 kg/s, volume flow rate $Q = 0.181$ m³/s, Mean velocity = 0.850 m/s. Top view

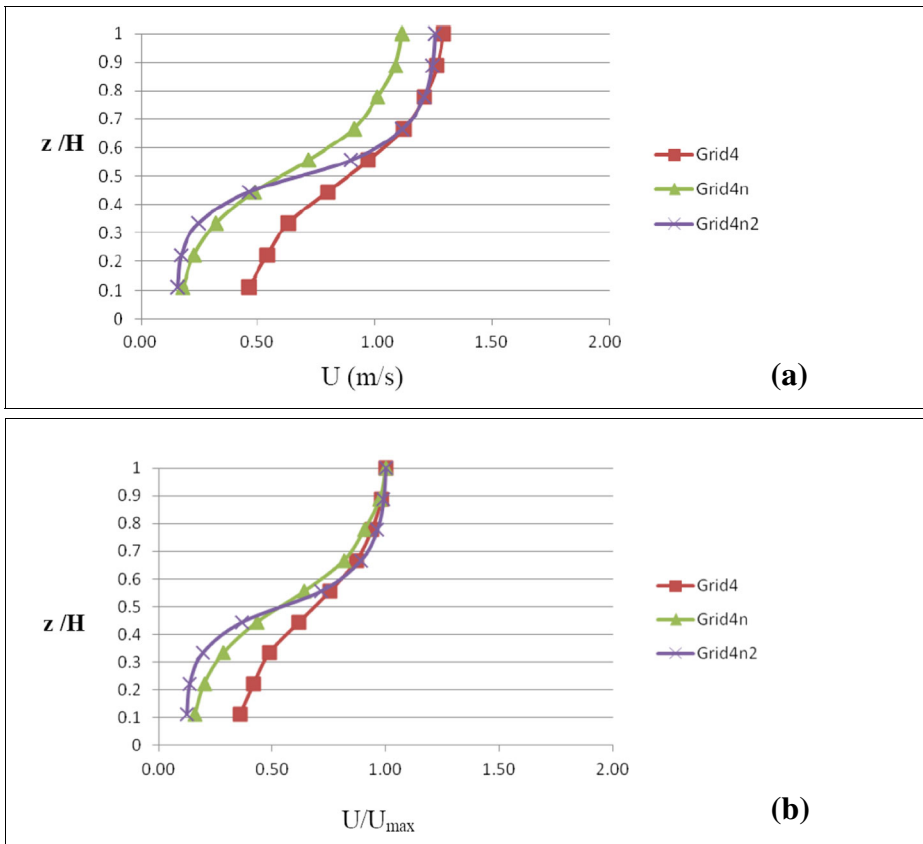


Fig. 6 Computed velocity profiles along the line segment (0,0,0) to (0,0,0.233 m). **a** Dimensional velocity, **b** Non-dimensionalized velocity

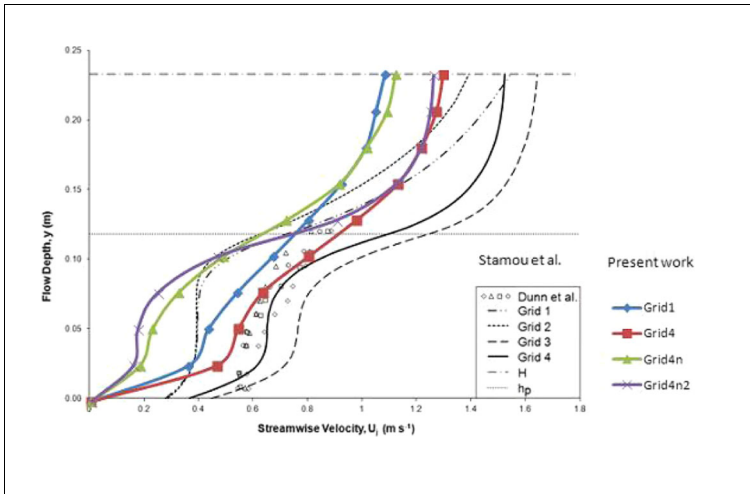


Fig. 7 Comparison of computed velocity profiles with calculated profiles by Stamou et al. (2012) and measurements by Dunn et al. (1996)

velocity the velocity at the top of the cylinders may be more appropriate (see Dunn et al. 1996). Furthermore, a test for convergence (when the mesh is refined) may be formulated by comparing profiles averaged in y for $x = \text{const}$.

The mean velocity profile is characterized by an inflection point (see Figs. 6 and 7). This type of profile is unstable according to the hydrodynamic stability theory of inviscid flow and leads to the development of Kelvin-Helmholtz vortices. These vortices are unsteady in nature and a time-dependent large eddy simulation (LES) simulation would be preferable to quantify this type of coherent flow structures. It is noted that the formation of coherent structures is a characteristic feature of the shear layer that develops in a horizontal zone $z_1 \leq z \leq z_2$ near the top of the rigid cylinders (Nepf and Ghisalberti 2008; Poggi et al. 2004). Our computed profiles exhibit essentially a three-layer structure which can be approximated by a hyperbolic tangent velocity distribution. The middle layer, which corresponds to the mixing layer in the model developed by Nepf and Ghisalberti (2008), is affected by the discontinuity in the drag and extends considerably below the top of the plant canopy.

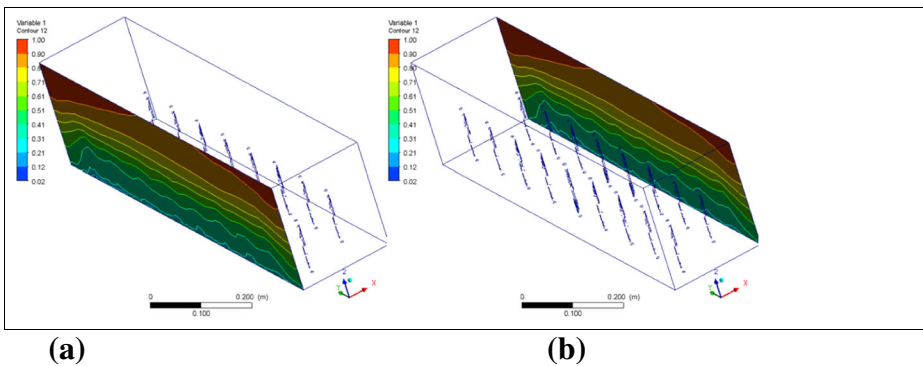
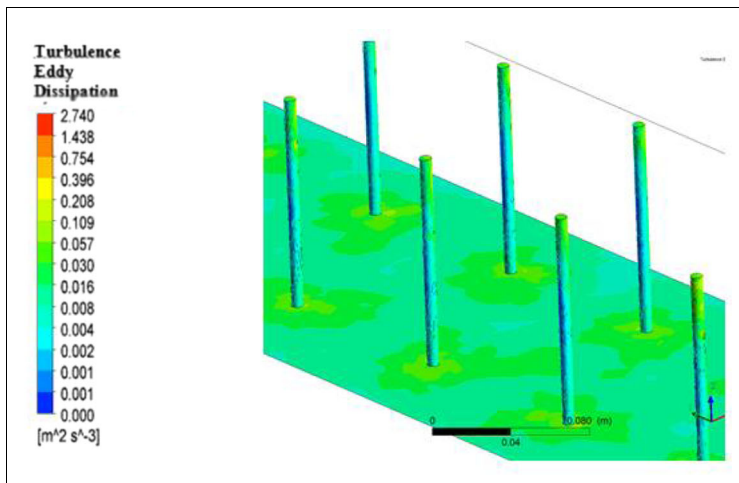
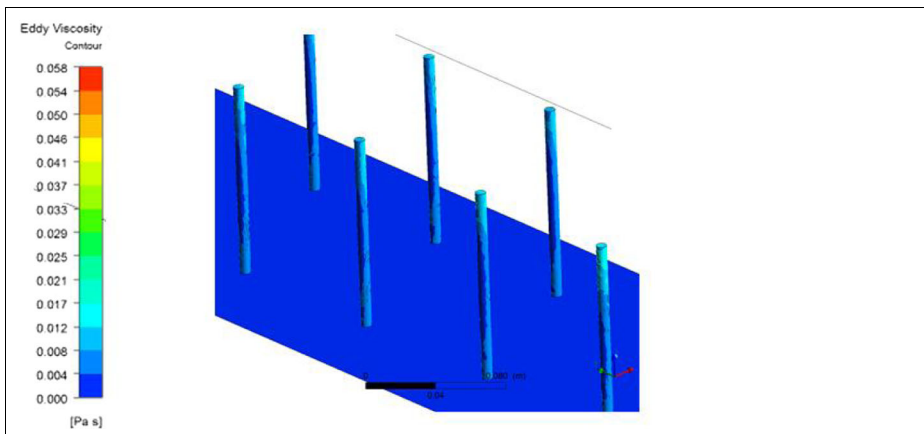


Fig. 8 Contour plot of the dimensionless velocity distribution profile: **a** on plane $x = -0.1016$ m; **b** on plane $x = 0.1016$ m. Mass flow rate: 141 kg/s, volume flow rate $Q = 0.141$ m³/s, Mean velocity = 0.662 m/s



(a)



(b)

Fig. 9 **a** Turbulence rate of dissipation, ε , and **b** Eddy viscosity at the rigid cylinder surfaces in a centered area of the channel far from the vertical side walls. Mass flow rate: 181 kg/s, volume flow rate $Q = 0.181 \text{ m}^3/\text{s}$, Mean velocity = 0.850 m/s

Typical dimensionless velocity contour plots are presented in Fig. 8. The dimensionless velocity helps us in the comparison of experimental and computational results obtained with fluids of different physical properties.

Turning now to the distribution of turbulence energy dissipation rate and eddy viscosity near the cylinders (Fig. 9), we observe that low values are detected near the bottom of the cylinders and higher as we move closer to the top of the cylinders. The last is probably observed due to the high shear stresses detected in this region.

In Fig. 10, eddy viscosity at different planes is presented. We observe that low values are detected at the central part of the channel and higher as we move near the solid side walls. In particular, we observe that near the vertical channel walls, regions of high eddy viscosity are present whose shape is greatly influenced by the presence of cylinders.

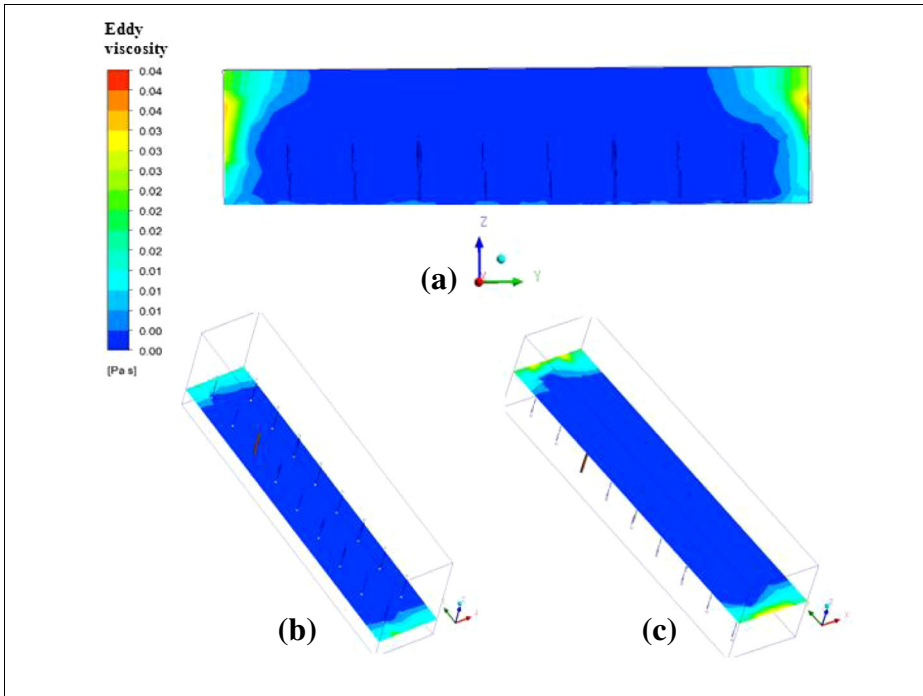


Fig. 10 Eddy viscosity at various planes: $x=0$, $z=0.05\text{m}$, $z=0.118\text{m}$. Mass flow rate: 201 kg/s , volume flow rate $Q = 0.201\text{ m}^3/\text{s}$, Mean velocity = 0.943 m/s

Regarding now the influence of the flow rate on the velocity pattern, we should comment that as the mass flow rate increases the layer thickness of the maximum velocity near the free surface also increases (compare Figs. 4 and 11). The flow pattern very close to the bottom of the channel is not greatly influenced at least for the range of volume flow rates studied in this work.

4 Conclusions

As noted in the introduction, the study of vegetated open channel flows has attracted considerable attention for many years. These flows are ubiquitous in nature and are characterized by high level of complexity. Historically, first hydraulic engineers focused on the estimation of increased resistance caused by the presence of vegetation in natural or man-made channels (Kouwen and Unny 1973; Kouwen 1992). Their objective was rather narrow and tried to obtain estimates of Manning coefficient, n , or equivalently the Darcy-Weisbach friction factor, f . Despite its empirical basis, this line of research is prerequisite for successful flood management (e.g., problems concerning the conveyance of flood waves). At the next level of complexity, fluid dynamical aspects of the flow, such as determination of mean flow velocity profiles as well as turbulence characteristics are studied. In this respect, fluid dynamicists followed work reported by meteorologists dealing with turbulence structure above terrestrial vegetation canopies (e.g., Finnigan et al. 2009). However, the hydraulic and fluid dynamical aspects are only “part of the problem”. Contaminant transport processes as well as sedimentation of suspended

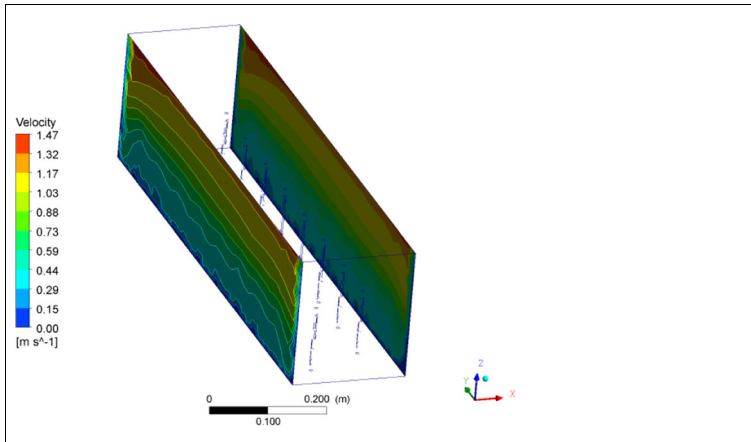


Fig. 11 Fluid speed distribution on planes $x = -0.1016$ m and $x = 0.1016$ m. Mass flow rate: 201 kg/s, volume flow rate $Q = 0.201$ m³/s, Mean velocity = 0.943 m/s

material are important processes in aquatic vegetation environments and have been studied by scientists concerned mainly about ecosystem management (Nepf and Ghisalberti 2008).

In this paper, we have presented simulations of turbulent flow in an open channel whose bed is covered with vegetation. The vegetation has been modeled by a series of small diameter rigid cylinders which protrude vertically from the channel bed. Calculations of velocity, kinetic energy, kinetic energy dissipation rate and eddy viscosity distribution on different plane sections show clearly that the presence of the vegetation affect considerably the fluid motion. As expected, vortices are formed in the wake region behind the cylinders. For the staggered arrangement of the cylinders and the distances among the cylinder (in multiples of cylinder diameters) studied, the interaction of the wakes is weak. The distribution of kinetic energy and kinetic energy dissipation rate on the cylinders reveal low values near the bottom of the channels which increase as we move at the top of the cylinders. Regarding eddy viscosity, it seems that low values are detected at the central part of the channel and they increase as we move near the solid walls. Moreover, it turns out that in the top and the bottom of the flow depth a “layer” of high eddy viscosity values exist whose pattern depends on the presence of the cylinders. The flow around the cylinder causes a force which is the resultant of the forces due to shear stresses and pressures on its surface. The total force is analyzed into two components, one parallel to the flow (roll resistance), and a component perpendicular to the flow called dynamic buoyancy of the cylinder. The cylinder resistance is due to frictional stresses on the surface and at different pressures as the height of the cylinder increases. The part of the resistance due to friction is called frictional resistance while the part of the resistance due to the different pressures along the cylinder is called form resistance. The effect of the flow rate on the velocity pattern is also investigated. The influence is detected mainly on the top of the vegetation where there is a maximum velocity layer whose thickness increases as the mass flow increases. Close to the bottom of the channel, the pattern is not greatly influenced from the flow rate, at least for the cases studied in this work.

The present study was carried out in order to develop tools for the calculation of the mean flow and turbulence characteristics which are important for understanding sediment transport and pollution process in floodplains. The effect of vegetation on quantities such as velocity, kinetic energy, kinetic energy dissipation rate and eddy viscosity distribution is significant and

should be further investigated with thicker vegetation stems, higher vegetation density and flexibility, on various conditions of channel bed. The authors believe that the present work constitutes a first step in the development of detailed flow models for flow in open channels with non-emergent vegetation. Incorporation of models of flexible plants will open the path for realistic modeling of sediment transport processes in vegetated floodplains as well as contaminant transport and dispersion. Looking forward, one envisages the use of such models for the design of macro-filters useful in environmental applications.

Acknowledgments An initial shorter version of the paper has been presented in Greek at the 3rd Joint Conference (13th of Hellenic Hydrotechnical Association, 9th of Hellenic Committee on Water Resources Management and 1st of the Hellenic Water Association) “*Integrated Water Resources Management in the New Era*”, Athens, Greece, December 10–12, 2015.

References

- ANSYS-CFX, Release 11.0 – User Guide
- Cui J, Neary VS (2008) LES study of turbulent flows with submerged vegetation. *J Hydraul Res* 46(3):307–316. doi:10.3826/jhr.2008.3129
- Defina A, Bixio AC (2005) Mean flow and turbulence in vegetated open channel flow. *Water Resour Res* 41:1–12. doi:10.1029/2004WR003475
- Dunn C, Lopez F, Garcia M (1996) Mean flow and turbulence in a Laboratory Channel with simulated vegetation. Hydrosystems Laboratory, Department of Civil Engineering, University of Illinois, Urbana-Champaign
- Erduran KS (2012) Integrated numerical model for vegetated surface and saturated subsurface flow interaction. *Appl Math Mech* 33(7):881–898. doi:10.1007/s10483-012-1592-9
- Finnigan JJ, Shaw RH, Patton EG (2009) Turbulence structure above a vegetation canopy. *J Fluid Mech* 637:387–424
- Fisher-Antze T, Stoesser T, Bates P, Olsen NRB (2001) 3D numerical modeling of open-channel flow with submerged vegetation. *J Hydraul Res* 39(3):303–310
- Huai WX, Zeng YH, Xu ZH, Yang ZH (2009) Three-layer model for vertical velocity distribution in open channel flow with submerged rigid vegetation. *Adv Water Resour* 32(4):487–492
- Katul GG, Poggi D, Ridolfi L (2011) A flow resistance model for assessing the impact of vegetation on flood routing mechanics. *Water Resour Res* 47:W08533
- Klopstra D, Barneveld HJ, Van Noortwijk JM, Van Velzen EH (1997) Analytical model for hydraulic roughness of submerged vegetation. Proceedings of the 27th IAHR Congress, San Francisco, pp775–780
- Kouwen N (1992) Modern approach to design of grassed channels. *J Irrigation and Drainage Engng* 118(5):713–728
- Kouwen N, Unny TE (1973) Flexible roughness in open channels. *J Hydraulic Div ASCE* 99(5):713–728
- Kucukali S, Cokgor S (2006) Discussion of open channel flow through different forms of submerged flexible vegetation by CAME Wilson, T Stoesser, PD Bates, a Batemann Pinzen. *J Hydraul Eng* 132:750–750
- Liakopoulos A (1985) Computation of high speed turbulent boundary-layer flows using the $k-\epsilon$ turbulence model. *Int J Numer Meth Fl* 5(1):81–97
- Liakopoulos A (2010) Fluid mechanics. Tziolas Publications (in greek)
- Liu D, Diplas P, Fairbanks JD, Hodges CC (2008) An experimental study of flow through rigid vegetation. *J Geophys Res* 113:F04015
- Lopez F, Garcia M (2001) Mean flow and turbulence structure of open channel flow through non-emergent vegetation. *J Hydraul Eng* 127(5):392–402
- Marjoribanks TI, Hardy RJ, Lane SN, Parsons DR (2016) Does the canopy mixing layer model apply to highly flexible aquatic vegetation? Insights from numerical modeling. *Environ Fluid Mech* 17:277–301
- Meijer DG, Van Velzen EH (1999) Prototype-scale flume experiments on hydraulic roughness of submerged vegetation. Proceedings of the XXVIII IAHR Congress, Graz
- Michalolias N (2014) The application of computational fluid dynamics in flood hazard management. Department of Civil Engineering, University of Thessaly, Diploma thesis (in Greek)
- Nepf H (2012) Hydrodynamics of vegetated channels. *J Hydraul Res* 50(3):262–279
- Nepf H, Ghisalberti M (2008) Flow and transport in channels with submerged vegetation. *Acta Geophysica* 56(3):753–777

- Nikora V (2010) Hydrodynamics of aquatic ecosystems: an interface between ecology, biomechanics and environmental fluid mechanics. *River Res Appl* 26(4):367–384
- Okamoto T-A, Nezu I (2010) Flow resistance law in open-channel flows with rigid and flexible vegetation. *River Flow* 261–268
- Poggi D, Porporato A, Ridolfi L (2004) The effect of vegetation density on canopy sub-layer turbulence. *Boundary Layer Meteorol* 111:565–587
- Stamou AI, Papadonikolaki G, Gkesouli A, Nikolettopoulos A (2012) Modeling the effect of vegetation on river floodplain hydraulics. *GNEST J* 14(3):371–377
- Stoesser T, Kim SJ, Diplas P (2010) Turbulent flow through idealized emergent vegetation. *J Hydraul Eng* 136:1003–1017
- Tsihrintzis VA, Madiedo EE (2000) Hydraulic resistance determination in marsh wetlands. *Water Resour Manag* 14(4):285–309
- Wilson CAME, Stoesser T, Bates PD, Batemann Pinzen A (2003) Open channel flow through different forms of submerged flexible vegetation. *J Hydraul Eng* 129(11):847–853
- Wilson CAME, Yagci O, Rauch HP, Olsen NRB (2006) 3D numerical modeling of a willow vegetated river/floodplain system. *J Hydrol* 327:13–21